Defect states in the high-dielectric-constant gate oxide La Al O 3

K. Xiong, J. Robertson, and S. J. Clark

Citation: Applied Physics Letters **89**, 022907 (2006); doi: 10.1063/1.2221521
View online: http://dx.doi.org/10.1063/1.2221521
View Table of Contents: http://scitation.aip.org/content/aip/journal/apl/89/2?ver=pdfcov
Published by the AIP Publishing

Defect states in the high-dielectric-constant gate oxide $LaAlO_3$

K. Xiong[a] and J. Robertson[b]
Engineering Department, Cambridge University, Cambridge CB2 1PZ, United Kingdom

S. J. Clark
Physics Department, Durham University, Durham, DH1 3HP, United Kingdom

(Received 27 March 2006; accepted 25 May 2006; published online 13 July 2006)

We present calculations of the energy levels of the oxygen vacancy, Al_{La} antisite, and oxygen interstitial defects in $LaAlO_3$ using density functional methods that do not need an empirical band gap correction. The levels are aligned to those of the Si channel using the known band offsets. The oxygen vacancy gives an energy level near the $LaAlO_3$ conduction band and above the Si gap. It is identified as the main electron trap and the cause of instability. The Al_{La} antisite gives a state near midgap, neutral when empty, which would be an important trap, with no counterpart in HfO_2.
 [DOI: 10.1063/1.2221521]

The continued scaling of complementary metal oxide semiconductor (CMOS) transistors requires the replacement of SiO_2 gate dielectrics by oxides of higher dielectric constant (κ) to minimize leakage currents.[1,2] Presently, the leading high *K* oxide is HfO_2. However, HfO_2 layers on Si tend to possess a SiO_2-based interfacial layer which limits the lowest effective oxide thickness (EOT) attainable. Future scaling calls for lower EOTs, and for this a leading candidate is $LaAlO_3$.[3–9] This is due to its higher *K*, lack of reactivity with Si, and larger band offsets with Si.[10–14] Critically, $LaAlO_3$ has much lower atomic diffusion rates and less tendency to form the SiO_2-based interfacial layer during processing.[15,16] Recently, amorphous $LaAlO_3$ gate stacks with an EOT of 0.3 nm have been achieved.[17]

Crystalline $LaAlO_3$(100) is lattice matched to Si(100), with a 45° lattice rotation, and it could grow as an epitaxial oxide.[3,13,18,19] However, presently $LaAlO_3$ films grown on Si are amorphous, unless a $SrTiO_3$ template layer is used. The amorphous phase has many advantages, over say HfO_2, as it does not crystallize until heated above 850 °C. Crystalline $LaAlO_3$ has a perovskite structure, like $SrTiO_3$. It differs from $SrTiO_3$ in that it is a 3-3 valent perovskite. As La and Al have the same valence, this means that La and Al antisites are possible defects and the ability of La and Al to mix sites could be why the films grow as an amorphous phase.

The introduction of high *K* oxides in CMOS has been delayed partly because of their high defect concentrations, particularly O vacancies, which result in charge trapping, transient threshold voltage shifts, and a degradation of Si carrier mobility due to remote Coulombic scattering. It is therefore important to have a good prediction of defect properties, particularly defect energy levels, as these determine the amount of any charge trapping. This letter presents calculations of the defect levels of $LaAlO_3$. For HfO_2, there have previously been calculations of the bulk, interfaces[20,21] and defect energy levels, using the generalized gradient approximation (GGA) of the local density approximation (LDA). However, LDA is well known to underestimate the band gap of insulators. It is possible to correct this empirically, but this is less reliable for gap states. It is preferable to use methods beyond the simple LDA which give correct band gaps.[22] These include GW approximation, B3LYP, LDA plus U, screened exchange (sX), and weighted density approximation (WDA). Here we use the sX and WDA methods,[23,24] as recently summarized.[22]

The calculations model the defect using the plane wave pseudopotential code CASTEP, a supercell of 40–80 atoms of cubic $LaAlO_3$, containing a single vacancy, interstitial, or antisite. The defect structures are relaxed in their various charge states using the PBE version of GGA using ultrasoft pseudopotentials. The defect energy levels are then calculated with the sX method, using norm-conserving pseudopotentials with a cutoff energy of 600 eV. The antisite and interstitial levels are also calculated in WDA with ultrasoft pseudopotentials and a cutoff of 400 eV. sX is more accurate than WDA, but WDA allows use of larger supercells, which are needed when there are large relaxations.

Figure 1 shows the band structure and partial density of states of bulk $LaAlO_3$. The valence band is formed of O 2*p* states, and the lowest conduction band is due to La *d* states with Al *s*,*p* states lying higher. The band gap of crystalline $LaAlO_3$ is calculated to be 3.1 eV in GGA, 4.4 eV in sX, and 6.7 eV in WDA, compared to 5.6 eV experimentally.[11,12] Unlike in HfO_2 where sX, WDA, and experimental gaps are similar, the sX gap of $LaAlO_3$ is smaller than the WDA or experimental gap.

Consider first the oxygen interstitial, denoted *I*. I^{2-}, the O^{2-} interstitial ion, is a closed shell system. It is spatially well separated from other O^{2-} ions. Its local density of states (DOS) shows that its energy levels lie inside the oxide valence band. The I^- or O^- ion behaves similarly to O^{2-}. It lies about 2 Å from other O^{2-} ions. The local DOS of O^- shows that it has a half-filled state about 0.5 eV above the valence band (VB) maximum. The I^0 or O^0 behaves differently. It has two holes and this allows it to form a dumbbell-shaped superoxyl ion O_2^{2-} with a direct O–O bond of length 1.453 Å, Fig. 2(a). This bond is shorter than the 1.49 Å for I^0 in HfO_2. The O–O bond lies at an angle of 64° to the Al–O–Al axis. Its DOS has an empty antibonding σ^* state at 4 eV in the upper gap, as in Fig. 2(b). There are also filled π and π^* states; the π^* state lies just above the VB edge. The I^+ ion is also possible, with a O–O bond of length 1.39 Å, giving a dumbbell shaped O_2^- ion. Its empty σ^* state is at 4.5 eV. It is

[a]Present address: IMEC, Kapeldreef 75, B-3001 Leuven, Belgium.
[b]Electronic mail: jr@eng.cam.ac.uk

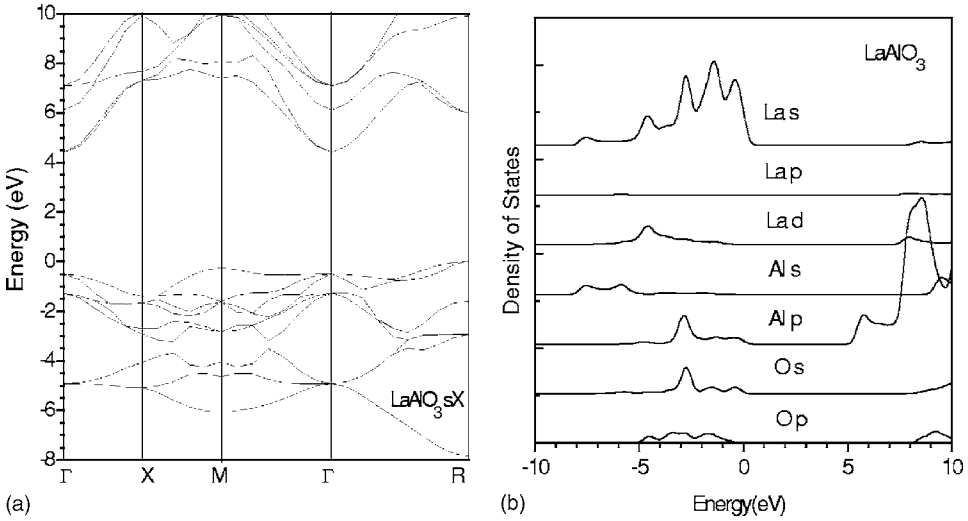

FIG. 1. (a) Band structure and (b) partial density of states of cubic $LaAlO_3$.

paramagnetic with a half-filled π^* state just above the valence band edge. Overall, the electronic states of the O interstitial are similar to those in HfO_2.[22]

Now consider the oxygen vacancy. In the perovskite lattice, an O ion is bonded to two Al ions. The neutral O vacancy V^0 creates a singly degenerate gap state of A_1 symmetry lying 0.8 eV below the conduction band in sX. It is occupied by two electrons for V^0. The state is strongly localized on the orbitals of the adjacent Al ions. The adjacent Al ions have a small outward relaxation of 0.06 Å for V^0. For the positive vacancies, V^+ and V^{2+}, the adjacent cations relax away from the vacancy site by 0.12 and 0.16 Å, respectively. The energy levels rise in the gap to lie at 0.6 and 0.55 eV, as shown in Fig. 3. Both are deep, but not as deep as the equivalent levels in HfO_2. Their energy levels are less dependent on the charge state or on relaxation than in HfO_2. Generally, the O vacancy is a shallower level in perovskites; it is a shallow donor in $SrTiO_3$, and only 0.5 eV deep in $PbTiO_3$.[25,26] The charge density of this A_1 defect state is plotted in Figs. 4(a) and 4(b) and it is strongly localized in the vacancy region.

The interesting aspect of V_O in HfO_2 was that it can also trap one or two electrons,[22,27] by undergoing a C_{2v} pairing distortion which pulls down an extra B_1 state from the Hf-like conduction band. In HfO_2, V_O is surrounded by four Hf's. In $LaAlO_3$, V_O has only two Al neighbors, and it cannot undergo such a distortion. Offering extra electrons to V_O just places them in delocalised conduction band states. There is no additional localized state. The A_1 state remains fully occupied and lies at 0.70 eV, and it has similar localization to those seen in Figs. 4(a) and 4(b).

The O vacancy was identified as the critical trapping center in HfO_2 and ZrO_2, because its A_1 level lies close to the Si band edge, and also the B_1 level is rather shallow,[22] and this causes a deleterious threshold voltage instability seen experimentally.[28,29] Processing should aim to minimize its effect. In $LaAlO_3$ V_O is shallower. Its energy levels can be aligned to those of the Si by using the conduction band offset of 1.8 eV.[13] This places the levels of V^0, V^+, and V^{2+} higher above the Si CB in $LaAlO_3$ than in HfO_2. This could lead to more trapping. But the absence of a V^- in $LaAlO_3$ is an advantage and should lessen the V_T instability.

A third type of defect occurs because $LaAlO_3$ is a 3-3 perovskite, and it is the antisite. The important antisite is Al at the La site, Al_{La}. Our calculations find that the neutral Al_{La} gives rise to an empty A_1 level in midgap, lying at about 4.4 eV in a 6.7 eV gap in WDA, or about 4.2 eV in a 6.0 eV gap. The defect level is a localized Al *s* state, as in Fig. 4(c). It arises because the atomic Al 3*s* orbital is much deeper than the La 5*s* orbital and is now not repelled out of the gap. This singly degenerate state of A_1 symmetry can take either one or two electrons to become negatively charged. The oxygens around the neutral Al_{La} relax inwards by 0.037 Å. The oxygens relax outwards by 0.02 Å at the negative antisite, a small relaxation.

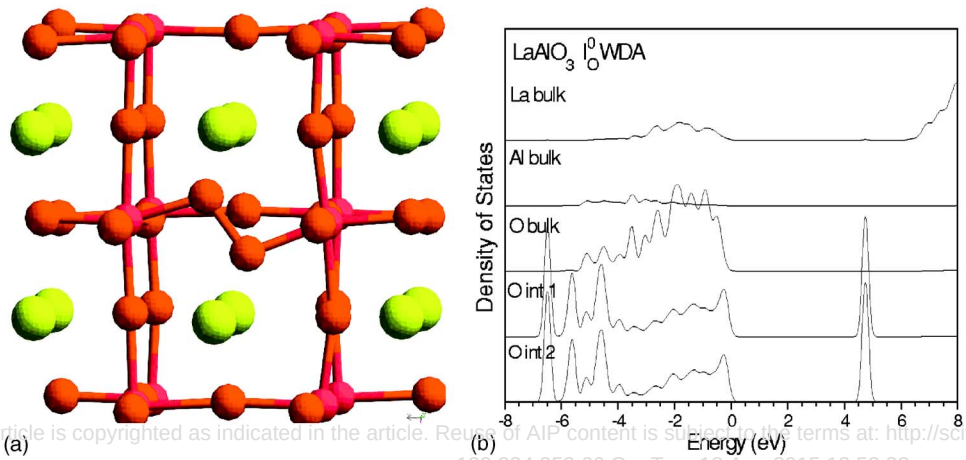

FIG. 2. (a) (Color online) Structure and (b) local density of states of the neutral interstitial oxygen site. Oxygen = red, Al = pink, La = yellow.

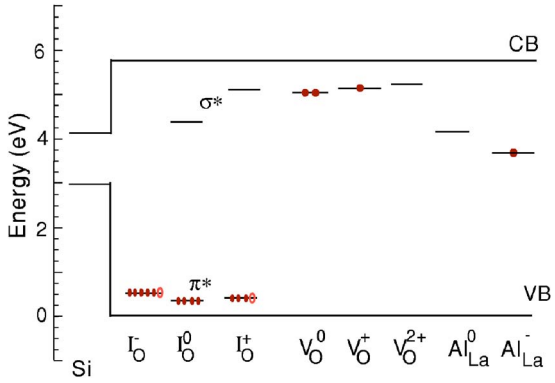

FIG. 3. Summary of energy levels of the O interstitial, O vacancy, and Al antisite in $LaAlO_3$ in their various charge states. Referred to the band edges of Si.

The key question is will any of these defects cause large voltage instabilities due to a high concentration. The formation energy of V_O in $LaAlO_3$ is large, as in HfO_2, but nevertheless a large, nonequilibrium concentration ($\sim 10^{19}$ cm^{-3}) of V_O occurs in HfO_2 in gate oxides, as they are seen in optical absorption spectra. This is due to the presence of reducing conditions and the adjacent gate metal.[30] For the same reasons, V_O will also be the key defect in $LaAlO_3$. The Al_{La} antisite could be problematic, due to its midgap state. There is also the question of how to define an antisite in amorphous $LaAlO_3$ and what their density will be. The formation energy of the neutral antisite in GGA is large, 6.8 eV, using the free energies of $LaAlO_3$, La_2O_3, and Al_2O_3 as reference. As this concentration is not dependent on the O chemical potential, we believe that the antisite concentration should be low ($<10^{16}$ cm^{-3}), so their effect will be low. There is no equivalent process, which creates nonequilibrium excess concentrations of the antisite, as there is for the O vacancy.

In conclusion, the energy levels of defects V_O, I_O, and the Al antisite are calculated. The O vacancy is identified as the critical defect. Its levels lie in the upper oxide band gap, about 0.7 eV deep, and above the Si CB. However, V_O does not possess a localized V^- level, which is the cause of transient trapping in HfO_2, so this could be beneficial. The Al antisite introduces a midgap state; however, it is likely to be present in low concentrations.

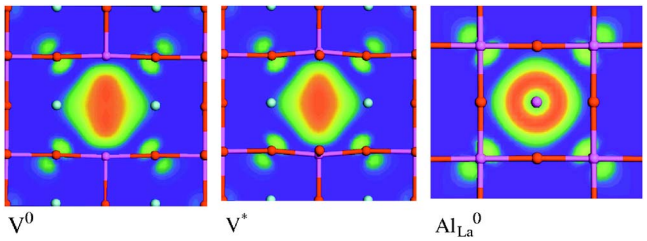

FIG. 4. (Color online) Charge density maps of the A_1 gap level of the V^0, and V^+ center, and the Al^0 antisite. Oxygen = red, Al = pink, La = blue.

[1]G. Wilk, R. M. Wallace, and J. M. Anthony, J. Appl. Phys. **89**, 5243 (2001).
[2]J. Robertson, Eur. Phys. J.: Appl. Phys. **28**, 265 (2004).
[3]B. E. Park and H. Ishiwara, Appl. Phys. Lett. **79**, 806 (2001); **82**, 1197 (2003).
[4]S. Gaillard, Y. Rozier, C. Merckling, F. Ducroquet, M. Gendry, and G. Hollinger, Microelectron. Eng. **80**, 146 (2005).
[5]R. A. B. Devine, J. Appl. Phys. **93**, 9938 (2003).
[6]X. B. Lu, Z. G. Liu, Y. P. Wang, Y. Yang, X. Wang, H. W. Zhou, and B. Nguyen, J. Appl. Phys. **94**, 1229 (2003).
[7]D. H. Triyoso, R. I. Hegde, J. M. Grant, J. K. Schaeffer, B. E. White, and P. J. Tobin, J. Vac. Sci. Technol. B **23**, 288 (2005); D. H. Triyoso, H. Li, R. I. Hegde, Z. Yu, K. Moore, B. E. White, and P. J. Tobin, *ibid.* **23**, 2480 (2005).
[8]B. S. Lim, A. Rahtu, P. Derouffignac, and R. G. Gordon, Appl. Phys. Lett. **84**, 3957 (2004).
[9]S. A. Shevlin, A. Curioni, and W. Andreoni, Phys. Rev. Lett. **94**, 146401 (2005).
[10]D. G. Schlom and J. H. Haeni, MRS Bull. **27**, 198 (2002).
[11]S. G. Lim, S. Kriventsov, T. N. Jackson, J. H. Haeni, D. G. Schlom, A. M. Balbashov, R. Uecker, P. Reiche, J. L. Freeouf, and G. Lucovsky, J. Appl. Phys. **91**, 4500 (2002).
[12]E. Cicerrella, J. L. Freeouf, L. F. Edge, D. G. Schlom, T. Heeg, J. Schubert, and S. A. Chambers, J. Vac. Sci. Technol. A **23**, 1676 (2005).
[13]L. F. Edge, D. G. Schlom, S. A. Chambers, E. Cicerrella, J. L. Freeouf, B. Hollander, and J. Schubert, Appl. Phys. Lett. **84**, 726 (2004).
[14]V. V. Afanasev, A. Stesmans, C. Zhao, M. Caymax, T. Heeg, J. Schubert, Y. Jia, D. G. Schlom, and G. Lucovsky, Appl. Phys. Lett. **85**, 5917 (2004).
[15]L. F. Edge, D. G. Schlom, R. T. Brewer, Y. J. Chabal, J. R. Williams, S. A. Chambers, Y. Yang, S. Stemmer, M. Copel, B. Hollander, and J. Schubert, Appl. Phys. Lett. **84**, 4629 (2004).
[16]P. Sivasubramani, M. J. Kim, B. E. Gnade, R. M. Wallace, L. F. Edge, D. G. Schlom, H. S. Craft, and J. P. Maria, Appl. Phys. Lett. **86**, 201901 (2005); L. Miotti, K. P. Bastos, C. Driemeier, V. Edon, M. C. Hugon, B. Agius, and I. J. R. Baumvol, *ibid.* **87**, 022901 (2005).
[17]M. Suzuki, M. Tomita, T. Yamaguchi, and N. Fukushima, Tech. Dig. - Int. Electron Devices Meet. **2005**, 445.
[18]D. O. Klenov, D. G. Schlom, H. Li, and S. Stemmer, Jpn. J. Appl. Phys., Part 2 **44**, L617 (2005).
[19]C. J. Forst, K. Schwarz, and P. E. Blochl, Phys. Rev. Lett. **95**, 137602 (2005).
[20]P. W. Peacock and J. Robertson, J. Appl. Phys. **92**, 4712 (2002).
[21]P. W. Peacock and J. Robertson, Phys. Rev. Lett. **92**, 057601 (2004).
[22]K. Xiong, J. Robertson, M. Gibson, and S. J. Clark, Appl. Phys. Lett. **87**, 183505 (2005).
[23]B. M. Bylander and L. Kleinman, Phys. Rev. B **41**, 7868 (1990).
[24]P. P. Rushton, D. J. Tozer, and S. J. Clark, Phys. Rev. B **65**, 235203 (2002).
[25]R. K. Astala and R. D. Bristowe, Modell. Simul. Mater. Sci. Eng. **12**, 79 (2004).
[26]K. Xiong and J. Robertson, Mater. Res. Soc. Symp. Proc. **902**, T8.4 (2005).
[27]Y. P. Feng, A. T. L. Lim, and M. F. Li, Appl. Phys. Lett. **87**, 062105 (2005).
[28]A. Kerber, E. Cartier, L. Pantisano, R. Degraeve, T. Kauerauf, Y. Kim, G. Groeseneken, H. E. Maes, and U. Schwalke, IEEE Electron Device Lett. **24**, 87 (2003).
[29]D. Felnhofer, E. P. Gusev, P. Jamison, and D. A. Buchanan, Microelectron. Eng. **80**, 58 (2005).
[30]E. P. Gusev, Tech. Dig. - Int. Electron Devices Meet. **2004**, 729.